

# Electrical Transport Properties of Superlattices under Intense Terahertz Electric Fields\*

P. S. S. Guimarães<sup>(a)</sup>, Brian J. Keay<sup>(b)</sup>, Jann P. Kaminski<sup>(b)</sup>, S. J. Allen, Jr.<sup>(b)</sup>,  
P. F. Hopkins<sup>(c)</sup>, A. C. Gossard<sup>(c)</sup>, L. T. Florez<sup>(d)</sup> and J. P. Harbison<sup>(d)</sup>

<sup>(a)</sup>Departamento de Física, Universidade Federal de Minas Gerais

Cx. Postal 702, 30161-970 Belo Horizonte, MG, Brasil

<sup>(b)</sup>Center for Free Electron Laser Studies

University of California, Santa Barbara, CA 93106, USA

<sup>(c)</sup>Materials Department University of California, Santa Barbara, CA 93106, USA

<sup>(d)</sup>Bellcore, Redbank, NJ 07701, USA

Received February 17, 1994

We report measurements of the low DC field conductance and the nonlinear IV characteristics of GaAs/AlGaAs multiquantum well superlattices submitted to intense AC electric fields in the terahertz frequency range. The DC conductance exhibits an oscillatory behavior as a function of the terahertz field strength that resembles the zero order Bessel function,  $J_0(edE/\hbar\omega)$ , where  $e$ ,  $d$ , and  $E$  are the electron charge, superlattice period and AC field strength respectively. The nonlinear DC IV characteristics display new steps and plateaus when the superlattices are subjected to the terahertz fields. The dependency of this new structure in the IV curves on frequency shows that the AC fields introduce new electronic conduction channels via photon mediated sequential tunneling.

## I. Introduction

The electrical transport properties of structures with a spatial periodicity subjected to intense submillimeter wave radiation have been extensively investigated theoretically. The simultaneous presence of strong spatial and temporal modulations is expected to lead to some striking effects. In fact, the original proposal of semiconductor superlattices<sup>[1,2]</sup> was motivated by the strong non-linear high frequency phenomena expected for such structures. Resonance-induced transparency effect was predicted by Ignatov and Romanov<sup>[3,4]</sup>. They calculated the high frequency electrical conductivity of superlattices and found that the current excited in a superlattice of spatial periodicity  $d$  by an AC field  $E = E_0 \cos(\omega t)$  is proportional to the zero order Bessel function  $J_0(\omega_B/\omega)$ , where  $\omega_B = eE_0d/\hbar$  is the Bloch frequency. Therefore, the current should vanish at the zeros of  $J_0$ , i.e., the superlattice is "transparent" for certain combinations of values of magnitude and frequency of electric field and superlattice period. Similar

calculations performed by Pavlovich and Épshtein<sup>[5,6]</sup> for superlattices submitted to both strong AC and DC electric fields show several regions of negative differential and absolute conductivities in the current-voltage characteristics.

The calculations mentioned above are based on a semi-classical description of superlattice transport<sup>[7]</sup>. A quantum mechanical treatment<sup>[8]</sup>, based on Floquet theory, shows a collapse of the superlattice minibands at certain values of AC electric field magnitude,  $E_0$ . The minibands widths are predicted to become close to zero at the same values of  $E_0$  where  $J_0(\omega_B/\omega)$  goes to zero. The appearance of Bessel functions with the given argument is ubiquitous to theories describing periodic structures in intense AC electric fields. This includes superlattices with minibands as well as those with thick potential barriers, in which the electrical transport occurs via sequential tunneling.

Most of the theoretical work on electrical transport in periodic structures submitted to intense high frequency fields has considered only the coherent tunneling case. An early work by Kazarinov and Suris<sup>[9]</sup>

\*Invited talk

analyses conduction in the sequential tunneling regime and it is predicted that under strong AC and DC fields one should obtain amplification of the electromagnetic wave for a certain range of frequencies. Otherwise, comparatively little attention has been paid to sequential tunneling in periodic structures under intense high frequency electric fields.

None of the theoretical predictions has been tested experimentally until now. The requirements for the experimental observation of the predicted phenomena are demanding. One needs intense and high frequency fields, that is, the conditions  $\omega\tau > 1$  and  $eE_0d/\hbar\omega \geq 1$  must be satisfied. For a semiconductor superlattice, in which typically  $d \simeq 10\text{nm}$  and  $\tau \simeq 10^{-12}\text{s}$ , electric field magnitudes in excess of  $10^3\text{kV/cm}$  are required for the near infrared and visible range. For frequencies in the far infrared,  $\omega \simeq 10^{12}\text{Hz}$ , the condition  $\omega\tau > 1$  is achieved but fields of the order of several  $\text{kV's/cm}$  are still needed. High power tunable sources in this frequency range are not readily available.

This paper describes an experimental investigation of electrical transport properties of semiconductor superlattices submitted to intense AC electric fields in the terahertz range of frequencies. Far infrared (FIR) radiation at the kilowatt power level was provided by the free electron lasers<sup>[10]</sup> of the Center for Free Electron Laser Studies at the University of California at Santa Barbara. As shown in the following, the terahertz radiation significantly affects the DC tunneling conductivity of the superlattices. At low bias the DC conductance exhibits an oscillatory behavior as a function of AC field strength that resembles the zero order Bessel function,  $J_0(\omega_B/\omega)$ . The nonlinear DC IV characteristics displays new steps and plateaus which are due to the introduction of new electronic conduction channels via photon mediated sequential tunneling.

## II. Device characteristics and experimental arrangements

The samples are GaAs/Al<sub>0.3</sub>Ga<sub>0.7</sub>As superlattices grown by molecular beam epitaxy (MBE). On a  $n^+$  GaAs substrate, doped with Si to  $1 - 2 \times 10^{18}\text{cm}^{-3}$ , the MBE layers are grown in the following sequence:

a 200nm thick GaAs buffer layer doped with Si,  $N_D = 2 \times 10^{18}\text{cm}^{-3}$ ; the superlattice, consisting of GaAs wells and AlGaAs barriers uniformly doped with Si with  $N_D = 2 - 3 \times 10^{15}\text{cm}^{-3}$ ; and a 100nm thick  $n^+$  GaAs cap layer, with Si doping  $N_D = 2 \times 10^{18}\text{cm}^{-3}$ . The width of the GaAs quantum wells in the superlattice is 25nm for sample 1, 33nm for sample 2, and 40nm for sample 3. The thickness of the AlGaAs barriers is 4nm, the same for the three samples. Samples 1 and 2 have 100 superlattice periods, i.e., 100 wells and barriers, while sample 3 has 50 periods.

For the electrical measurements, square mesas  $200\mu\text{m}$  on a side were defined by standard photolithographic techniques and shallow AuGeNi ohmic contacts were alloyed on the mesa top as well as the substrate. Gold wires of  $25\mu\text{m}$  diameter were bonded to each contact. The experiments were performed over a temperature range 2-300 K.

The far infrared radiation from the free electron lasers was coupled to the superlattices using the gold wire bonded to the top contact as an antenna. The angle of incidence and polarization direction of the radiation with respect to the antenna were carefully adjusted for each experiment in order to maximize the coupling efficiency. The strength of the coupling can be qualitatively judged by looking at the size of the FIR-induced changes in the sample conductivity. However, there is no quantitative measurement of the coupling strength and the absolute magnitude of the AC electric fields in the superlattice structure is not known. For the free electron lasers used in this work, typical maximum power levels are of the order of several kilowatts at 600 GHz, which focused to a few square mm's will generate free space electric fields of the order of several kilovolts/cm. It is assumed that the terahertz electric field in the superlattices is of this order of magnitude.

At temperatures below approximately 100K, the vertical electrical transport in all three superlattices occurs via the sequential tunneling mechanism. Fig. 1 shows the DC current-voltage (I-V) characteristics of the three superlattices at low temperatures. The I-V characteristics for each structure are essentially independent of temperature below 100K. The curves show the sequence of steps and plateaus characteristic of the sequential tunneling regime<sup>[11]</sup>. At the lowest biases the current through the superlattice is controlled by se-

quential resonant tunneling from the ground state of one well of the superlattice to the ground state of the neighboring well. As the bias, and so the current, increases, this conduction channel saturates. Further increases in the applied voltage will lead to the formation of a high field domain in which the conduction occurs via tunneling from the ground state in one well to the first excited state in the neighboring well, followed by an intra-well relaxation of energy from the excited to the ground state. Due to charge accumulation in the wells, the electric field is not uniform but increases from the negatively biased side of the sample to the positive contact. Therefore, the high field domain will appear in the quantum well next to the positive contact. The high field domain expands with increasing bias until it takes over the whole sample. At this point there is again just one conduction mechanism through the whole sample, the tunneling/relaxation process involving the ground and first excited states of the quantum wells. With increasing bias, this mechanism also saturates and similar processes will occur involving higher excited quantum well states and leading to additional steps in the I-V characteristic.

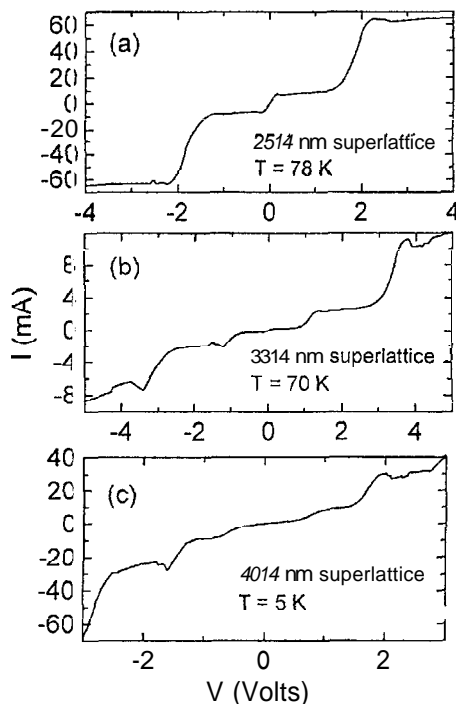


Figure 1: The current-voltage (I-V) characteristics of the samples measured at low temperatures, in the range in which conduction is primarily via sequential resonant tunneling. (a) Sample 1, 25nm quantum wells; (b) sample 2, 33nm wells; and (c) sample 3, 40nm wells.

### III. Fir-induced changes in the low bias conductivity

Figs. 2, 3 and 4 show the dependence of the low bias DC conductivity of the samples on the magnitude of the terahertz electric field. The DC conductivity was measured applying a constant DC bias to the superlattice and looking for the change in the DC current across the sample when in the simultaneous presence of the high frequency electric field supplied by the free electron laser. The DC bias was chosen in the region where the electronic conduction is via sequential tunneling from ground state in one well to ground state in the next well, i.e., before the first plateau in the I-V characteristic. Care was taken to eliminate the small photo-voltaic current resulting from partial rectification of the AC field due to the intrinsic asymmetry of the structure and the electrical contacts. The results shown are essentially the same for all temperatures below approximately 100K (in the sequential tunneling regime).

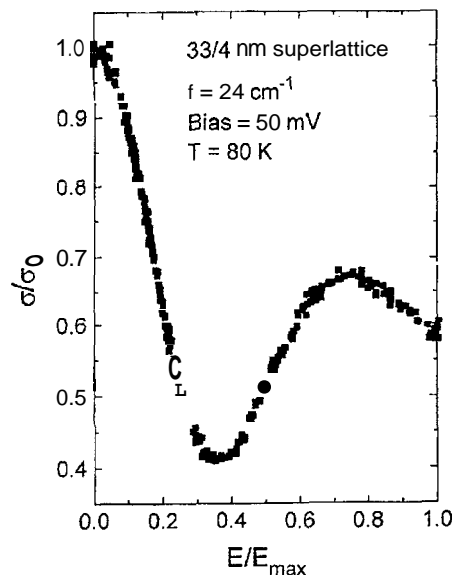


Figure 2: The DC conductivity of the 33nm wells, 4nm barriers superlattice, as a function of the magnitude of the AC electric field. The conductivity is normalized to the conductivity at zero AC field and it is measured with a constant DC bias of 50mV applied to the sample. The frequency of the AC field is  $7.2 \times 10^{11}$  Hz ( $24\text{cm}^{-1}$ ).

The terahertz field clearly has a strong effect on the DC conductivity. For the 33/4nm superlattice (Fig. 2), the conductivity first drops with increasing AC field strength to about 40% of its value in the dark,  $\sigma_0$ , then

risers to around 70% of  $\sigma_0$  and decreases again to  $0.6\sigma_0$  at the highest attainable AC electric field magnitude. A similar, even more pronounced oscillatory behavior is seen for the 40/4nm structure (Fig. 3). For the 25/4nm superlattice (Fig. 4), it seems that the AC field is not strong enough to reveal the oscillations in the conductivity but there is indication that if a higher AC field magnitude could be achieved, this sample would also show the oscillatory behavior seen in Figs. 2 and 3.

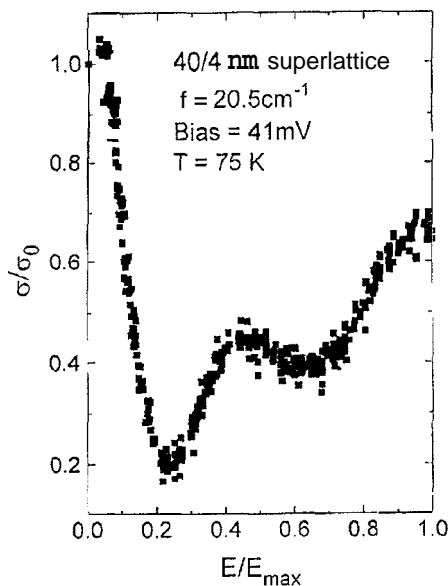


Figure 3: The DC conductivity of the 40nm wells, 4nm barriers superlattice, as a function of the magnitude of the AC electric field. The conductivity is normalized to the conductivity at zero AC field and it is measured with a constant DC bias of 41mV applied to the sample. The frequency of the AC field is  $6.1 \times 10^{11}$  Hz ( $20.5\text{cm}^{-1}$ ).

The oscillating conductivity shown in Figs. 2-4 resemble the Bessel function behavior predicted by the theories mentioned in the introduction. The estimated AC field magnitudes in the samples are adequate to produce this result. A tentative fit of the experimental curves with Bessel functions of order zero displaced from the horizontal axis has moderate success. It could be that experimental problems like parallel conduction or variation of coupling strength of the laser radiation with its magnitude are distorting the shape of the conductivity versus AC field magnitude curve.

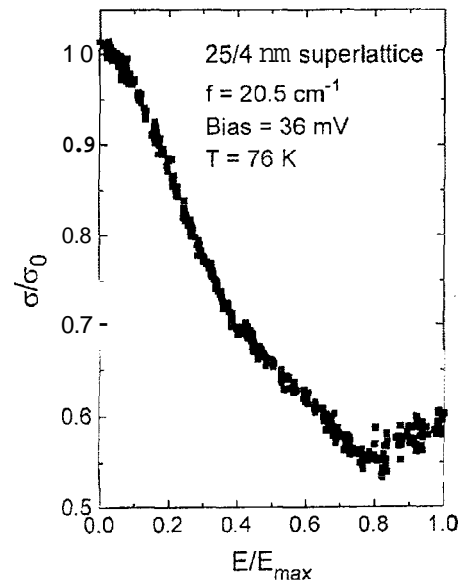


Figure 4: The DC conductivity of the 25nm wells, 4nm barriers superlattice, as a function of the magnitude of the AC electric field. The conductivity is normalized to the conductivity at zero AC field and it is measured with a constant DC bias of 36mV applied to the sample. The frequency of the AC field is  $6.1 \times 10^{11}$  Hz ( $20.5\text{cm}^{-1}$ ).

Alternatively, it is possible that the oscillations in the superlattice potential due to the AC field lead to the oscillations in the conductivity. As the AC field magnitude is increased, the overlap in energy of the ground state in one well with the ground state in the neighboring wells, averaged over one period of the laser radiation, will decrease. Therefore, the tunneling probability decreases and the conductivity drops. The conductivity will rise again when the time-averaged overlap in energy between energy levels in neighboring wells increases. This should happen whenever the amplitude of the AC electric field is such that the maximum potential drop caused by the AC field across one period of the superlattice is equal to the separation in energy between the ground and one of the excited states of the quantum wells. The resonant tunneling probability, and so the conductivity, should then oscillate with increasing terahertz field magnitude. The separation between the peaks in the conductivity will consequently be determined by the separation in energy of the quantum states in the multi-quantum well superlattice.

To test this hypothesis, one would need to know the absolute value of the AC field magnitude in the superlattice. As mentioned before, this can only be estimated since the coupling strength of the radiation to the sam-

ple is unknown. One possibility is to check if in the different samples, with different quantum well thicknesses and energy level positions (which can be easily calculated) the oscillations in the conductivity scale as implied by this model. However, for this test to be a quantitative one, one would have to assume that the coupling strength is the same for all samples, which is almost certainly not true. Qualitatively, though, the position of the conductivity oscillations do scale as expected. Note that the oscillations have the smallest period in the 40/4nm structure (Fig. 3), where the separation between the quantum well energy levels is smallest. For the 25/4nm superlattice (Fig. 4), where the energy levels are well spaced, apparently the highest achieved AC field magnitude is just enough to make the maximum potential drop caused by the AC field across one period of this superlattice equal to the separation in energy between the ground and first excited state. The 33/4nm structure is intermediate between these two cases. Further work is necessary to test this model.

#### IV. Photon-assisted sequential resonant tunneling

The results discussed above concern the terahertz field-induced changes in the DC conductivity at a constant low bias applied to the superlattice, in the ground state to ground state resonant tunneling regime. Fig. 5 shows the I-V characteristic of sample 2 (33nm wells/4nm barriers) under laser radiation of different frequencies, for a temperature of 75K. These results are essentially temperature independent below approximately 100K, i.e., in the sequential resonant tunneling regime<sup>[12]</sup>.

It is clear in Fig. 5 that the terahertz radiation produces new steps and plateaus in the I-V characteristic. The position in voltage of the new steps is a function of the frequency, with the onset of the new plateaus moving to lower voltages as the frequency increases. The onset of the new plateaus also depends weakly on the far infrared radiation intensity.

The frequency dependence of the onset of the new plateaus induced by the terahertz radiation in the I-V

curve is shown in Fig. 6. The voltage position of the onset of a new plateau was defined as the position of the minimum in the  $\partial^2 I / \partial V^2$  curve in the region of voltage where the new step appears. The voltage shown in the y-axis is the total voltage applied to the superlattice divided by 100, the number of periods of the structure. The solid lines in the figure are best straight line fits through the data plotted as open squares.

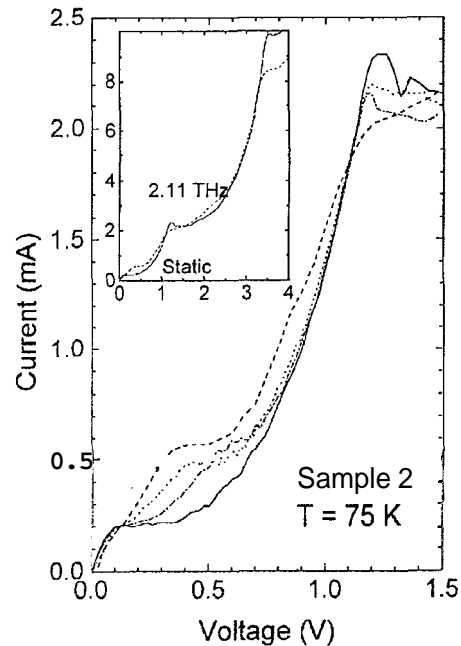


Figure 5: The dependence of the DC current-voltage characteristics of the 33nm wells/4nm barriers multi-quantum well superlattice on the frequency of the AC electric field. The static I-V characteristic (solid line) is shown again for comparison. For clarity, only three frequencies are shown: 1.50 THz (dash-dotted line), 1.83 THz (dotted line) and 2.11 THz (dashed line). The inset is an extended view of the static and 2.11 THz I-V curves showing the additional structure around 2.1V.

There are some striking features in Fig. 6. First, most of the data, plotted as open squares, lie along straight lines that have slopes  $\Delta V / \Delta f = -h/e$ , to within the experimental error. Here,  $h$  is Planck's constant and  $e$  is the magnitude of the electron charge. Second, the  $f = 0$  intercepts of these lines, 11.8meV and 30.6meV, correspond closely to the calculated energy separations between the ground state,  $\epsilon_0$ , and the first,  $\epsilon_1$ , and second,  $\epsilon_2$ , excited states, respectively. Using a simple envelope function approximation in the absence of a DC electric field, we obtain  $\epsilon_1 - \epsilon_0 = 12.4\text{meV}$  and  $\epsilon_2 - \epsilon_0 = 32.7\text{meV}$ . The only data that do not lie on these straight lines, plotted as closed circles on Fig. 6,

are the ones for  $f = 3.1$  to  $3.3$  THz. These frequencies correspond closely to the energy difference between the ground and first excited states. Clearly, some different process is occurring for the highest frequencies, involving laser-induced transitions between these two states.

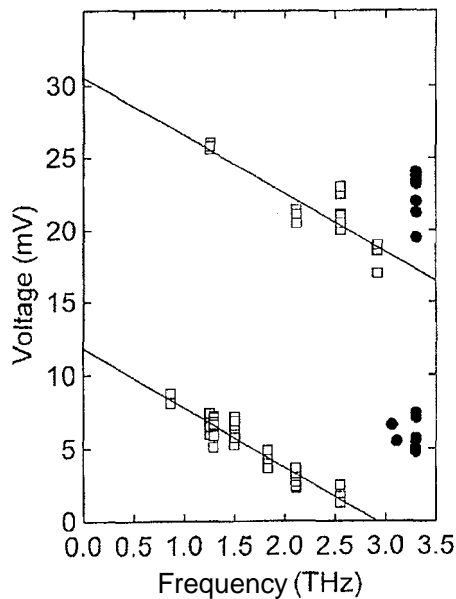


Figure 6: The voltage positions of the onset of the AC field-induced plateaus in the I-V characteristic of the 33nm wells/4nm barriers multi-quantum well superlattice plotted as a function of the frequency of the far infrared field. The voltages shown are the voltage drops across a single period of the superlattice if a uniform DC electric field is assumed.

The straight line behavior shown in Fig. 6 strongly suggests that the new structure induced in the I-V characteristic by the terahertz radiation is due to photon-mediated-tunneling<sup>[12-14]</sup> and that the DC voltage is dropped uniformly across the sample, at these bias points, in the presence of the intense terahertz radiation. The far infrared electric field opens a new conduction channel, in which an electron can tunnel from the ground state in one quantum well to an excited state  $\epsilon_n$  in the neighboring well with the absorption of a photon. The electron then releases the excess energy  $eV = (\epsilon_n - \epsilon_0)$  in an intra-well transition to the ground state and a new photon-mediated tunneling process to the next quantum well follows.

The new steps in the I-V curves occur at voltage biases where the static conditions necessitated high electric field domains. These domains will be altered only when the new conduction channels are strong enough to dominate the transport. The photon-assisted tunneling

model exposed above implies that the terahertz fields are sufficiently strong to make photon-mediated tunneling a significant mechanism of electronic conduction, at least around the DC biases where the new structure in the I-V curve is observed. This is consistent with the significant changes in current induced by the AC field at these biases. The conclusion from the data is that the terahertz radiation forces a uniform distribution of the applied DC voltage at these positions in bias. It is possible that some of the power dependency of the data points in Fig. 6 is due to residual field inhomogeneities. Generally, the new steps in the I-V curve appear at slightly higher DC bias as the intensity of the laser field is increased.

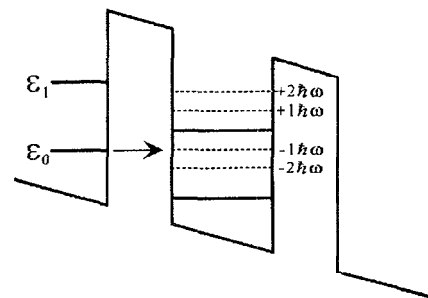


Figure 7: The photon assisted tunneling process viewed as tunneling from one well into photon sidebands of a state in the neighboring well.

A clear view of how the photon-assisted tunneling process gives rise to the new steps and plateaus in the I-V curves is provided by the concept of photon sidebands<sup>[15]</sup>, as shown schematically in Fig. 7. The new steps are due to processes similar to the ones that produce the plateaus in the static characteristic, except that the tunneling is from the ground state in one well to a photon sideband in the neighboring well. The two lines in Fig. 6 correspond to tunneling from the ground state of one well to photon sidebands of the first and the second excited states in the adjacent well. Note that only processes involving photon absorption are seen. It is not clear why processes involving photon stimulated emissions are not observed.

## V. Conclusion

In conclusion, it was shown in this paper that intense AC electric fields in the terahertz range of frequencies substantially affect the DC conductivity of

multiquantum well semiconductor superlattices at low temperatures. For low DC biases, when the electronic conduction in the structure is via sequential resonant tunneling from the ground state of one well to the ground state of the adjacent well, the DC conductance exhibits an oscillatory behavior as a function of the terahertz field intensity which resembles the zero order Bessel function which appears in theories describing transport, properties of periodic structures submitted to intense AC electric fields. The dependency of the DC I-V characteristics of the superlattices on the frequency of the AC radiation shows that the terahertz fields introduce a new mechanism of electronic conduction, photon-mediated sequential tunneling.

#### Acknowledgments

The experiments reported here were made possible by the commitment, knowledge and skill of the staff at the UCSB Center for Free Electron Laser Studies, J.R.Allen, D.Enyeart, G.Ramian, D.White and B.Wallace. This work was performed while P.S.S.G was visiting the CFELS supported by a grant from CNPq, Brazil. B.J.K was partially supported by the USA NSF Science and Technology Center for Quantized Electronic Structures Grant No. DMR 91-20007. P.F.H. and A.C.G. were supported by the USAF Office of Scientific Research Grant No. AFOSR-91-0214. The CFELS is supported by the USA Office of Naval Research (N00014-92-J-1452).

#### References

1. L. Esaki and R. Tsu, IBM J. Res. Dev. 14, 61 (1970).
2. R. Tsu and L. Esaki, Appl. Phys. Lett. 19, 246 (1971).
3. A. A. Ignatov and Yu. A. Romanov, Sov. Phys. Solid State 17, 2216 (1976).
4. A. A. Ignatov and Yu. A. Romanov, Phys. Stat. Sol. (b) 73, 327 (1976).
5. V. V. Pavlovich and É. M. Épshtein, Sov. Phys. Semicond. 10, 1196 (1976).
6. V. V. Pavlovich and É. M. Épshtein, Sov. Phys. Solid State 18, 863 (1976).
7. For a review see F. G. Bass and A. P. Tetervov, Phys. Rep. 140, 237 (1986).
8. M. Holthaus, Phys. Rev. Lett. 69, 351 (1992).
9. R. F. Kazarinov and R. A. Suris, Sov. Phys. Semiconductors 6, 120 (1972).
10. G. Ramian, Nuclear Instr. Meth. Phys. Res. A318, 225 (1992).
11. K. K. Choi, B. F. Levine, R. J. Malik, J. Walker and C. G. Bethea, Phys. Rev. B 35, 4172 (1987).
12. P. S. S. Guimarães, Brian J. Keay, Jann P. Kaminski, S. J. Allen, Jr., P. F. Hopkins, A. C. Gossard, L. T. Florez and J. P. Harbison, Phys. Rev. Lett. 70, 3792 (1993).
13. V. A. Chitta, R. E. M. de Bekker, J. C. Maan, S. J. Haworth, J. M. Chamberlain, M. Henini and G. Hill, Surface Sci. 263, 227 (1992).
14. V. A. Chitta, R. E. M. de Bekker, J. C. Maan, S. J. Haworth, J. M. Chamberlain, M. Henini and G. Hill, Sem. Science and Tech. 7, 432 (1992).
15. P. K. Tien and J. P. Gordon, Phys. Rev. 129, 647 (1963).